Properties of resonance states in H^-

C. D. Lin
Center for Astrophysics, Harvard College Observatory and Smithsonian Astrophysical Observatory, 60 Garden St., Cambridge, Massachusetts 02138
(Received 2 February 1976)

Using hyperspherical coordinates and a Born-Oppenheimer–type expansion, the potential curves of H^- that converge to the $n = 1$ and $n = 2$ thresholds of hydrogen are obtained. From the computed potential curves, the properties of bound states, Feshbach resonances, and shape resonances are conveniently studied.

I. INTRODUCTION

The existence of resonances in electron-hydrogen scattering was first indicated from the three-state close-coupling calculation by Burke and Schey[1] in 1962. Since then, many theoretical methods[2] have been employed to obtain the positions and widths of these resonance states. The results of these calculations are in harmony with existing experimental data.

Most of these methods are based either upon close-coupling expansion[3] of the total two-electron wave function in terms of target eigenfunctions or upon the Feshbach projection operator which separates the elastic scattering channel from the total scattering eigenfunctions.[4] The actual calculations used in these methods are essentially variational in nature, and very often only a few quantities can be extracted from a large calculation. The dynamic correlation between the two electrons which determines the computed values is not studied.

Recently, we used hyperspherical coordinates to study the electron-hydrogen system,[5-7] with the spirit of solving the two-electron Schrödinger equation directly. The method is designed such that some meaningful intermediate results can be studied. Interesting results have thus been obtained. In particular, we have been able to trace the origin of the difference in the autoionization rates of the doubly excited states of helium.[5] Quantitatively, this approach also gives a fairly good result for the bound-state energy of H^- and the $^1S^e$ elastic electron-hydrogen scattering phase shifts.[6] In a recent communication,[7] the author has shown that the $^1P^o$ Feshbach and shape resonances of H^- can be predicted accurately using this approach. In the present paper we describe the calculational methods used and give a detailed analysis of the other resonances in H^- lying below the $n = 2$ threshold of the hydrogen atom.

In hyperspherical coordinate system, the position of the two electrons with respect to the nucleus is treated as a point in six-dimensional space $\{R, \alpha, \theta_1, \phi_1, \theta_2, \phi_2\}$, with $R = (r_1^2 + r_2^2)^{1/2}$ and $\alpha = \arctan(r_2/r_1)$, where r_1 and r_2 are the distances of the two electrons from the nucleus and (θ_1, ϕ_1) and (θ_2, ϕ_2) are the usual spherical angles. In this coordinate system, R measures the size and $\Omega \equiv \{\alpha, \theta_1, \phi_1, \theta_2, \phi_2\}$ denotes the orientation of the whole system and of their relative positions.[8] Since the angular coordinates are confined to finite ranges, the kinetic energy (velocity) associated with angular motion is larger (faster) than that associated with radial motion.[9] This is particularly true at small R, because the kinetic energy associated with angular motion is scaled as $1/R^2$ and that associated with radial motion is d^2/dR^2. The fast angular motion produces an effective potential for the radial motion. Thus we treat this problem in a manner analogous to diatomic molecular problems by expanding the total wave function as $\psi(R, \Omega) = \sum_\mu F_\mu(R)\Phi_\mu(R; \Omega)$,[10] where $\Phi_\mu(R; \Omega)$ is similar to the electronic wave function at a fixed internuclear distance R and $F_\mu(R)$ is similar to the vibrational wave function in the diatomic case. In the first approximation, the couplings between radial and angular motions are neglected.

The properties of angular wave functions $\Phi_\mu(R; \Omega)$ and their associated potentials $U_\mu(R)$ have been studied in I for He.[5] The qualitative behavior of $\Phi_\mu(R; \Omega)$ in H^- is not much different from that in He, but the shape of $U_\mu(R)$ is very different because the interaction in the asymptotic region (at large R) is different. Section II presents the numerical method used in this calculation and its comparison with other methods used in previous calculations. The resulting potential curves and computed eigenvalues for the resonances are presented in Sec. III for $^{1,3}S^e$ and $^{1,3}P^o$ states. From these curves several misconceptions about H^- are pointed out; they resulted from numerical artifacts by using very simple and limited trial wave functions in the variational calculations. In particular, we conclude that except the ground state there is no

other possible bound state of H^- associated with the $n=1$ limit of H. Also, there is no other possible shape resonance associated with the $n=2$ threshold of H except the $^1P^o$ shape resonance discussed in Ref. 7. This last conclusion differs from the recent results of Herrick,[11] where a $^3P^o$ shape resonance is reported. Finally, the potential curve associated with the nonautoionizing $2P^2\,^3P^e$ state is computed. This state is only barely bound; its position is obtained by applying effective range theory.

II. NUMERICAL METHODS

For each total orbital and spin angular momentum L, S and parity π, the two-electron wave function $\psi(R,\Omega)$ is expanded as

$$\psi(R,\Omega)=(1/R^{5/2})\sum_{\mu} F_\mu(R)\Phi_\mu(R;\Omega). \tag{1}$$

Substituting (1) into the Schrödinger equation in hyperspherical coordinates, a system of coupled differential equations

$$\left(\frac{d^2}{dR^2}-U_\mu(R)+2E\right)F_\mu(R)+\sum_{\mu'\neq\mu}W_{\mu,\mu'}(R)F_{\mu'}(R)=0 \tag{2}$$

is obtained. (Atomic units are used throughout this paper unless otherwise indicated.) In Eq. (2), the diagonal coupling term $W_{\mu,\mu}(R)$ (which is often neglected in the molecular calculation) and a factor $3.75/R^2$ resulting from elimination of the d/dR term in (2) are included in the definition of the potential $U_\mu(R)$ in each channel, i.e., $U_\mu(R)=V_\mu(R)-W_{\mu,\mu}(R)+3.75/R^2$, where $V_\mu(R)$ is obtained by solving

$$[(\Lambda^2-RC)/R^2]\Phi_\mu(R;\Omega)=V_\mu(R)\Phi_\mu(R;\Omega) \tag{3}$$

at each R. Explicit expression and detailed discussions of the coupling term $W_{\mu,\mu'}$, the generalized angular momentum operator Λ and the total Coulomb interaction $-C/R$ are given in I. Equation (3) is an eigenvalue partial differential equation which has been solved using three different methods. In the following, we give a brief description of, and some comments on, each method.

1. Diagonalization. This method is used in I and has been used by other workers in related problems. Essentially, one uses the eigenfunctions of the Λ^2 operator as basis functions to evaluate the matrix elements of C. The eigenvalues of (3) at each R are obtained by diagonalizing the resulting matrix of (3). This method is efficient at small R, where reasonable accuracy can be achieved by using a limited number of basis functions. However, at modest and large R, where the α-dependent part of the angular function $\Phi_\mu(R;\Omega)$ approaches hydrogenic behavior, the diagonalization method is very inefficient, because a large number of basis functions[5] (whose α-dependent part is proportional to Jacobi polynomials) are needed. The slow convergence is also encountered in the variational calculations of the helium ground-state energy done recently be other workers.[12] This method serves the purpose of I because only qualitative features of $\Phi_\mu(R;\Omega)$ at small R are studied. In Ref. 6, this numerical difficulty is somewhat avoided in ^1S because of symmetry.[13]

2. Numerical integration. The partial differential equation (3) is reduced to a system of coupled equations in α at each R by expanding $\Phi_\mu(R;\Omega)$ as

$$\Phi_\mu(R;\Omega)=\sum_{l_1l_2} g_\mu^{(l_1l_2)}(R;\alpha)\mathcal{Y}_{l_1l_2LM}(\hat{r}_1\hat{r}_2), \tag{4}$$

and by integrating over spherical angles $\hat{r}_i \equiv(\theta_i,\phi_i)$. In Eq. (4), the expansion into partial angular momentum (l_1, l_2) can be truncated to only a few pairs for the low-lying excited states studied here,[14] each pair coupled to total angular momentum L described by $\mathcal{Y}_{l_1l_2LM}(\hat{r}_1,\hat{r}_2)$. This method was used by Macek[10] to calculate the potential curves for helium. The eigenvalues are obtained by imposing appropriate boundary conditions at $\alpha=0^\circ$ and 45° for each L, S and π. This method is accurate, but the eigenfunction $\Phi_\mu(R;\Omega)$ cannot be studied easily.

3. Finite-difference method. This method is used in the present calculation as well as in Ref. 7. Here, $\Phi_\mu(R;\Omega)$ is expanded as

$$\Phi_\mu(R;\Omega)=\frac{1}{\sqrt{2}}\sum_{[l_1l_2]}\left[g_\mu^{(l_1l_2)}(R;\alpha)\mathcal{Y}_{l_1l_2LM}(\hat{r}_1\hat{r}_2)+(-1)^{l_1+l_2-L+S}g_\mu^{(l_1l_2)}(R;\tfrac{1}{2}\pi-\alpha)\mathcal{Y}_{l_2l_1LM}(\hat{r}_1\hat{r}_2)\right]. \tag{5}$$

In (5), the proper symmetry for each L, S, π is written down explicitly for each (l_1l_2), and the summation in (5), unlike in (4), is over pairs of l_1l_2 only, i.e. $[l_1l_2]$ is not different from $[l_2l_1]$. By substituting (5) into (3), we obtain a system of coupled equations as in method (2), except that the structure is different. Explicitly, we get

$$\left(\frac{d^2}{d\alpha^2} - \frac{l_1(l_1+1)}{\cos^2\alpha} - \frac{l_2(l_2+1)}{\sin^2\alpha} + R^2 V_\mu(R)\right) g_\mu^{(l_1 l_2)}(R;\alpha)$$

$$+ R \sum_{[l_1' l_2']} \left[C_{l_1 l_2, l_1' l_2'}(\alpha)\, g_\mu^{(l_1' l_2')}(R;\alpha) + (-1)^{l_1'+l_2'-L+S} C_{l_1 l_2, l_1' l_2'}(\alpha)\, g_\mu^{(l_1' l_2')}(R;\tfrac{1}{2}\pi-\alpha)\right] = 0, \quad (6)$$

where

$$C_{l_1 l_2, l_1' l_2'}(\alpha) = \langle \mathcal{Y}_{l_1 l_2 L M}(\hat{r}_1, \hat{r}_2) | C | \mathcal{Y}_{l_1' l_2' L M}(\hat{r}_1, \hat{r}_2) \rangle .$$

For $l_1 \neq l_2$, the number of coupled equations in (6) is half of that in method (2). These coupled equations are most conveniently solved using finite differences. If a second-difference method is used, an ordinary differential equation is reduced to a symmetric tridiagonal matrix. Very accurate eigenvalues can be obtained if the mesh size is sufficiently small and extrapolation to zero mesh size is used.[15] In Eq. (6), if only one $[l_1 l_2]$ component with $l_1 \neq l_2$ is retained, the resulting matrix is not tridiagonal but has skew-diagonal terms originating from $g_\mu^{(l_1 l_2)}(R; \frac{1}{2}\pi - \alpha)$. The matrix form of the general coupled equations (6) can be separated into blocks, each diagonal block having the structure described above for each $[l_1 l_2]$. The off-diagonal block between $[l_1 l_2]$ and $[l_1' l_2']$ has nonzero matrix elements along the diagonal and skew-diagonal only. When $l_1 = l_2$, all of the skew-diagonal matrix elements mentioned above also vanish. In the present calculations, two different mesh sizes are used at each R. Choosing 45–60 points within $0 \leq \alpha \leq 90°$, the adopted eigenvalues V_μ at each R are obtained by extrapolation using a quadratic expansion in h, $E_h = V_\mu + bh^2$, where E_h is the computed eigenvalue from matrix diagonalization when the mesh size is h. This method is very easy to program and is efficient provided a suitable diagonalization subroutine is available for a sparse matrix. In the present calculation, we use a general diagonalization subroutine for symmetric matrices, as no more suitable programs are available. Therefore the present calculation is limited to include only two sets of $[l_1 l_2]$. This is adequate for the cases studied below.

III. RESULTS AND DISCUSSIONS

A. Elastic scattering channels

The lowest $^{1,3}S^e$ and $^{1,3}P^o$ potential curves of H^- that converge to the ground state of H at large R are shown in Fig. 1. Each corresponds to an effective potential seen in the elastic e-H scattering at that particular L, S and π. Only the $^1S^e$ curve shows an attractive well at small R; this potential well is strong enough to support a bound state, corresponding to the ground state of H^-. Results of the computed ground-state energy and elastic phase shifts were previously reported in good agreement with other calculations. From the computed $^1S^e$ curve, we conclude that only one bound state can be supported, arguing either from the value of the WKB phase integral near the ionization limit[16] or from Levinson theorem[17] applied to the phase shifts computed from this curve.[6] The smooth $^1S^e$ curve also rules out any possible shape resonances near the $n=1$ threshold. The so-called $1s2s\,^1S$ state of H^- reported by Rudkjøbing and coworkers[18] can in all likelihood therefore be attributed to numerical artifacts arising from the rough variational wave functions used. Our conclusion is in agreement with the majority of other, more sophisticated calculations and with experiments.[19] Similarly, the potential curves for $^3S^e$ and $^{1,3}P^o$ states shown in Fig. 1 also exclude any possibility of bound states or resonances near the $n=1$ threshold of H. Again, the so-called $1s2s\,^3S^e$ and $1s2p\,^{1,3}P^o$ states computed by Rudkjøbing and coworkers[18] are probably due to numerical artifacts. It must be pointed out that our methods do not assume the existence of any bound states or resonances prior to the calculation, in contrast with variational calculations where unphysical results may emerge from calculations if unphysical constraints are imposed on the trial wave functions. Furthermore, the existence of resonances, however narrow, should be evident from the computed potential curves. An example of this is the $^1P^o$

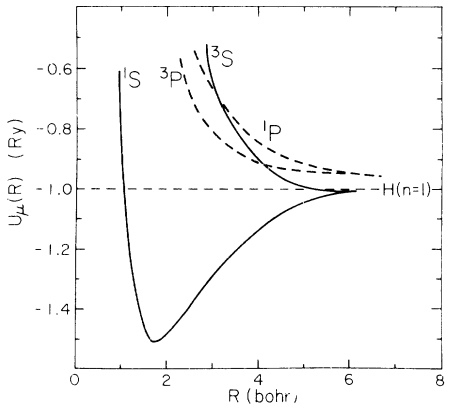

FIG. 1. Potential curves of H^- that converge to the ground state of the hydrogen atom.

shape resonance above the $n=2$ limit of H reported in Ref. 7. This is in contrast to the close-coupling-type calculation where a narrow resonance may escape notice if the phase shifts are not computed at closely spaced energy points.

It is interesting to note that the shape of the $^1S^e$ and $^3S^e$ curves shown in Fig. 1 are very similar to the familiar $^2\Sigma_g^+$ and $^2\Sigma_\mu^+$ curves of H_2^+. Actually, the origin of the shapes of potential curves in these two cases is identical. In H_2^+, the repulsive $^2\Sigma_\mu^+$ curve results from the antisymmetric character of the electronic wave function, with a node midway between the nuclei. In the ^3S state, the repulsive behavior of the potential curve comes from the antisymmetry requirement of $\Phi_\mu(R;\Omega)$, with a node at $\alpha=45°$ for every R.

The elastic phase shifts computed from the $^3S^e$ and $^{1,3}P^o$ curves are not as accurate as those determined from other variational calculations. For these systems, the electron-electron correlation effects are not very important since the electrons do not penetrate effectively near the nucleus together and thus do not interact strongly. In such systems, calculations starting with a single-particle model are often more accurate. We can improve the computed elastic phase shifts by including the coupling terms $W_{\mu,\mu'}$ with higher curves.[6]

B. Doubly excited channels

The two curves of $^{1,3}S^e$ and the three curves of $^{1,3}P^o$ states of H^- that converge to the $n=2$ limit of H at large R are shown in Fig. 2. The properties implied by the $^1P^o$ curves and the crossing between the curves designated by "+" and "−" are reported in Ref. 7.

It is noted that the $^1S^e$ and $^3P^o$ curves are more attractive than the corresponding $^3S^e$ and $^1P^o$ curves. At large R, the asymptotic potentials are determined by the dipole interactions owing to hydrogenic $2s$ and $2p$ degeneracy, and the asymptotic potentials are spin independent. The $\mu=2$ curve of $^3S^e$ and the "−" curve of $^1P^o$ at large R are attractive because of dipole interactions. At small R, the depths of the attractive potential wells are manifestations of electron-electron correlation. As pointed out in I, the "+" curves of $^{1,3}P^o$ have characteristics similar to the attractive ^1S curves; this feature is seen in Fig. 2 by noting the attractive potential wells at small R. However, as explained in Ref. 7, the "+" and "−" curves of $^3P^o$ do not cross and the "−" curve in this case is completely repulsive, similar to the pd curves of $^{1,3}P^o$. An obvious conclusion from these $^3P^o$ curves is that there is no shape resonance associated with $^3P^o$ near the $n=2$ threshold of H, a result in contradiction to the recent conclusion of Herrick,[11] where a shape resonance is reported. This is an indication of the inadequacy of the group-theoretical approach to such systems. Our conclusion in this regard agrees with the results of close-coupling calculations.

The eigenvalues and radial wave functions for each asymptotic attractive potential curve $U_\mu(R)$ of Fig. 2 are obtained by solving

$$\left(\frac{d^2}{dR^2}-U_\mu(R)+2E\right)F_\mu(R)=0\,. \tag{7}$$

The lowest eigenvalue for each curve is shown by a horizontal line in Fig. 2, and the eigenfunctions are plotted in Fig. 3. Note that the lowest $^1S^e$ and $^3P^o$ states, to be called $2s^2\,^1S^e$ and $2s2p\,^3P^o$, respectively, are localized at a much smaller R. The radius of the lowest $^3S^e$ and $^1P^o$ states are localized at approximately the same radius, thus justifying the designation $(2s3p\text{-}2p3s)^1P^o$ for this state. Other higher eigenvalues are shown in

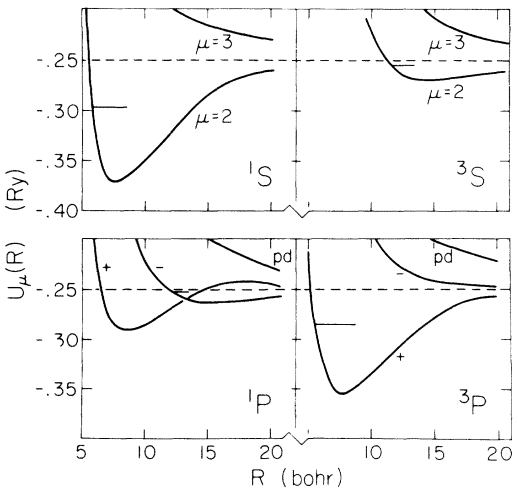

FIG. 2. Potential curves of H^- that converge to the $n=2$ level of the hydrogen atom.

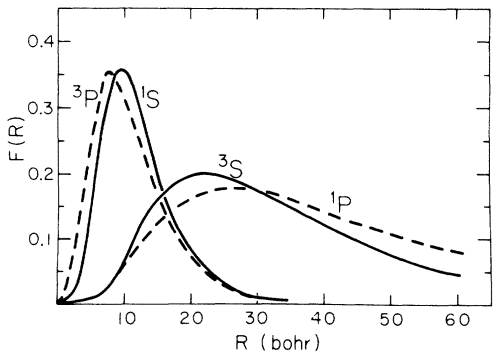

FIG. 3. Radial wave functions of the lowest Feshbach resonance states of Fig. 2.

TABLE I. Energy levels of H^-. All energies are given in eV with respect to the ground state of the hydrogen atom. Energies given in the first two columns do not include shifts due to the interaction with the continuum, while the values in the last two columns have the shifts included. Correction for the finite mass of the nucleus is employed in the conversion from rydbergs to electron volts, with 1 Ry = 13.5984 eV.

		This work	OG [a]	3CCC [b]	BT [c]
^1S	E_1	9.560	9.554	9.555	9.555
	E_2	10.175	10.173	10.173	
	E_3	10.197			
^3S	E_1	10.145	10.144	10.145	
	E_2	10.196	10.1977		
^1P	E_1	10.173	10.173		
	E_2	10.198	10.198		
^3P	E_1	9.719	9.722	9.735	9.738
	E_2	10.189	10.193		
	E_3	10.198			

[a] O'Malley and Geltman, Ref. 4.

[b] Three-state close-coupling calculations with 20 correlation terms (Ref. 2).

[c] Projection operator method of Bhatia and Temkin, Ref. 25.

Table I, together with results from other calculations. Our results for $^1S^e$ are too high compared with others. This is because d^2 partial waves are not included in this calculation.[10]

The asymptotic attractive potentials of Fig. 2 can be represented by $-a^2/R^2$ from the $n=2$ threshold of H. If the potential is of this form for all R, then the one-dimensional Schrödinger equation has analytical solutions,[21] its successive eigenvalues given by the recursion relation

$$E_{n+1} = E_n e^{-2\pi/\alpha}, \tag{8}$$

where $\alpha = (a^2 - \frac{1}{4})^{1/2}$. For the attractive potentials of Fig. 2, the approximation $-a^2/R^2$ is valid only for $R > R_0$, with $R_0 \simeq 20$. The higher eigenvalues of H^- should also be related by Eq. (8) for sufficiently large n. The condition for (8) to be valid is $\frac{1}{2}|E_n|R_0^2 \ll 1$,[20] corresponding to $|E_n| < 10^{-3}$ Ry. Therefore the states which lie less than 10^{-3} Ry below the $n=2$ limit are related by Eq. (8) if they belong to the same series. By comparing with the computed eigenvalues of Table I, we notice that Eq. (8) can be applied for all $n \geq 1$ of $^3S^e$ and $^1P^o$ states, and for all $n \geq 2$ of $^1S^e$ and $^3P^o$ states. Temkin and Walker[20] used Eq. (8) to find the higher eigenvalues of H^-, with E_n taken from the *lowest* computed eigenvalues of O'Malley and Geltman[4] for each L, S and π. Thus the higher eigenvalues for $^1S^e$ and $^3P^o$ they obtained from Eq. (8) disagree with the values computed by O'Malley and Geltman.[4]

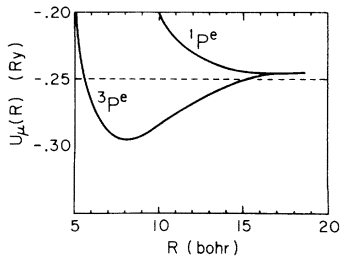

FIG. 4. Potential curves of $^{1,3}P^e$ states that converge to the $n=2$ level of hydrogen atom.

C. Ground channels of $^{1,3}P^e$

The lowest potential curves of $^{1,3}P^e$ states which converge to the $n=2$ limit of H are shown in Fig. 4. Only $(l_1 l_2) = (1,1), (2,2)$ are included in the calculation. Both curves behave asymptotically as $2/R^2$ as the result of the centrifugal potential of the outer electron. At small R, the $^1P^e$ curve is completely repulsive but the $^3P^e$ curve forms a shallow potential well. The behavior of the potential curves in Fig. 4 is very similar to the $^1S^e$ and $^3S^e$ curves of Fig. 1. In fact, the origin is the same. For the $^3P^e$ curve, the angular wave function $\Phi_\mu(R;\Omega)$ has an antinode at $\alpha = 45°$, similar to the ^1S curves, whereas for the $^1P^e$ curve, its $\Phi_\mu(R;\Omega)$ has a node at $\alpha = 45°$, analogous to the $^3S^e$ curves.

The shape of the $^3P^e$ curve is very similar to the "+" ^1P curve shown in Fig. 2; both have a shallow potential well at small R and a repulsive $2/R^2$ potential at large R. It was shown in Ref. 7 that the "+" curve is strong enough to support only a shape resonance. It is interesting to see if the $^3P^e$ curve can have a bound state. The possible eigenvalues of such a potential cannot be obtained

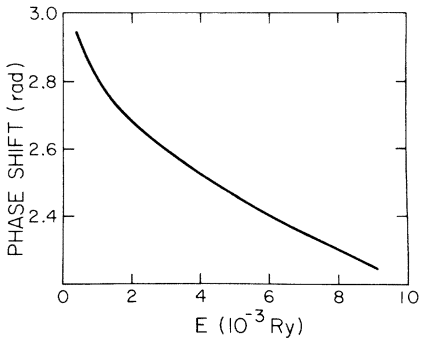

FIG. 5. Phase shifts computed from the $^3P^e$ curve of Fig. 4.

accurately by the usual numerical integration methods. We have tried using a finite-difference method[21] without success, because the state, if bound, is very diffuse and near threshold. We use an alternative method here. In Fig. 5 we show the computed phase shifts from this curve. This plot is very different from Fig. 2(a) of Ref. 7, even though the two potentials are very similar. The phase shifts of Fig. 5 can be extrapolated to a value near π at threshold. According to Levinson's theorem, this implies that the $^3P^e$ potential can support a bound state. The position of this bound state can be easily obtained by using effective range theory.[22] The value thus obtained is -7.5×10^{-4} Ry, which is to be compared with the Hylleraas-type variational result -7.0×10^{-4} Ry of Drake[23] and of Bhatia.[24]

---

[1]P. G. Burke and H. M. Schey, Phys. Rev. 126, 147 (1962).

[2]For recent reviews, see P. G. Burke, Adv. At. Mol. Phys. 4, 173 (1968); G. J. Schulz, Rev. Mod. Phys. 49, 378 (1973); J. S. Risley, in *Atomic Physics 4*, edited by G. Zu. Putlitz, E. W. Weber, and A. Winnacker (Plenum, New York, 1975), p. 487.

[3]For close-coupling calculations, see references quoted in P. G. Burke's article (Ref. 2). A variation of the close-coupling method employs pseudostate expansion; see, e.g., P. G. Burke, D. F. Gallaher, and S. Geltman, J. Phys. B 2, 1142 (1969).

[4]This method has been used by many authors where the open channel is projected out using the well-known P operator given by Y. Hahn, T. F. O'Malley, and L. Spruch, Phys. Rev. 128, 932 (1962). See, e.g., T. F. O'Malley and S. Geltman, Phys. Rev. 137, A1344 (1965); K. T. Chung and J. C. Y. Chen, Phys. Rev. A 6, 686 (1972); A. K. Bhatia and A. Temkin, Phys. Rev. A 8, 2184 (1973), and references quoted therein. They differ mainly only in the way of solving the closed-channel equations. All these authors either do not calculate the energy shift due to the interaction between the closed-channel and open channel, or they have to do an elaborate calculation. A different approach was used by G. W. F. Drake and A. Dalgarno, Proc. R. Soc. A 320, 549 (1971), where the Q operator is defined in terms of zeroth-order hydrogenic wave functions, an equation is derived where the intersection with the continuum is effectively included and the equation is then solved accurately by a $1/Z$ expansion.

[5]C. D. Lin, Phys. Rev. A 10, 1986 (1974), henceforth to be called I.

[6]C. D. Lin, Phys. Rev. A 12, 493 (1975).

[7]C. D. Lin, Phys. Rev. Lett. 35, 1150 (1975).

[8]In the classical three-body problem, one would like to eliminate the three angles, e.g., the Euler angles that describe the orientation of the whole system in space, and reduce the five angles to only two. However, in the quantum three-body problem, there is no advantage in doing this, because the Euler angles are coupled to other internal angles when the wave function is properly antisymmetrized. See A. K. Bhatia and A. Temkin, Rev. Mod. Phys. 36, 1050 (1964).

[9]For details, see U. Fano and C. D. Lin, in *Atomic Physics 4*, Ref. 2.

[10]J. H. Macek, J. Phys. B 1, 831 (1968).

[11]D. R. Herrick and O. Sinanoğlu, Phys. Rev. A 11, 97 (1975); D. R. Herrick, Phys. Rev. A 12, 413 (1975).

[12]D. L. Knirk, J. Chem. Phys. 60, 66 (1974). P. Cavaliere, G. Ferrante, R. Geracitano, and L. Lo Cascio, J. Chem. Phys. 63, 624 (1975). In order to achieve faster convergence, it is simpler and quicker to use polynomials of $\sin\alpha$ and of $\cos\alpha$ instead of the Jacobi polynomials [D. L. Knirk (private communication)], because the latter oscillate violently in the interval $0\le\alpha\le\frac{1}{2}\pi$. To expand a smooth function at large R in terms of these rapidly oscillating functions is impractical, because it requires many terms. This is the reason for the slow convergence in these calculations.

[13]For the ^1S state, the basis functions U_{llm} of I are limited to even values of m because of symmetry and the size of the matrix to be diagonalized at each R is reduced.

[14]U. Fano, J. Phys. B 7, L401 (1974).

[15]N. W. Winter, D. Diestler, and V. McKoy, J. Chem. Phys. 48, 1879 (1968). L. Fox, *Numerical Solution of Two-point Boundary Problems* (Oxford U. P., London, 1957).

[16]The WKB phase evaluated at 5.0×10^{-6} Ry below threshold is 2.49, nowhere close to the value $\frac{3}{2}\pi$ if a second bound state is nearby.

[17]See B. H. Bransden, *Atomic Collision Theory* (Benjamin, New York, 1970), p. 48.

[18]M. Rudkjøbing, Appl. Space Sci. 3, 102 (1969); J. Quant. Spectrosc. Radiat. Transfer 13, 1479 (1973), and references therein.

[19]C. L. Pekeris, Phys. Rev. 126, 1470 (1962), shows that $1s2s\ ^1S$ is not bound. Papers cited in Ref. 3 show no resonances exist near the gound state of H. To prove that $1s2s\ ^1S$ does not exist is very important, because the diffuse interstellar absorption lines at 4436, 4890, and 6180 Å have been attributed to autoionizing states of H^-. A recent photodetachment experiment on H^- by E. Herbet, T. A. Patterson, D. W. Norcross, and W. C. Lineberger, Astrophys. J. 191, L143 (1974), shows that the cross section is smooth near 4890 and 4430 Å, thus ruling out H^- as a possible candidate for these diffuse lines.

[20]A. Temkin and J. F. Walker, Phys. Rev. 140, A1520 (1965); P. M. Morse and H. Feshbach, *Method of Theoretical Physics* (McGraw-Hill, New York, 1953), p. 1665.

[21]F. L. Tobin and J. Hinze, J. Chem. Phys. 63, 1034 (1975).

[22]T. F. O'Malley, L. Spruch, and L. Rosenberg, J. Math. Phys. 2, 491 (1961).

[23]G. W. F. Drake, Phys. Rev. Lett. 24, 126 (1970).

[24]A. K. Bhatia, Phys. Rev. A 2, 1667 (1970).

[25]A. K. Bhatia and A. Temkin, Phys. Rev. A 11, 2018 (1975).